Universality class of site and bond percolation on multifractal scale-free planar stochastic lattice

M. K. Hassan and M. M. Rahman
Department of Physics, University of Dhaka, Dhaka 1000, Bangladesh
(Received 28 April 2016; revised manuscript received 1 August 2016; published 10 October 2016)

In this article, we investigate both site and bond percolation on a weighted planar stochastic lattice (WPSL), which is a multifractal and whose dual is a scale-free network. The characteristic property of percolation is that it exhibits threshold phenomena as we find sudden or abrupt jump in spanning probability across p_c accompanied by the divergence of some other observable quantities, which is reminiscent of a continuous phase transition. Indeed, percolation is characterized by the critical behavior of percolation strength $P(p) \sim (p_c - p)^{\beta}$, mean cluster size $S \sim (p_c - p)^{-\gamma}$, and the system size $L \sim (p_c - p)^{-\nu}$, which are known as the equivalent counterpart of the order parameter, susceptibility, and correlation length, respectively. Moreover, the cluster size distribution function $n_s(p_c) \sim s^{-\tau}$ and the mass-length relation $M \sim L^{d_f}$ of the spanning cluster also provide useful characterization of the percolation process. We numerically obtain a value for p_c and for all the exponents such as β, ν, γ, τ, and d_f. We find that, except for p_c, all the exponents are exactly the same in both bond and site percolation despite the significant difference in the definition of cluster and other quantities. Our results suggest that the percolation on WPSL belongs to a new universality class, as its exponents do not share the same value as for all the existing planar lattices. Besides, like all other cases, its site and bond type belong to the same universality class.

DOI: 10.1103/PhysRevE.94.042109

I. INTRODUCTION

Percolation is perhaps one of the most studied problems in statistical physics. This is not only because of the simplicity of its definition but also because of the versatility of its applications. To study percolation one first needs to choose a skeleton. It can be a lattice or a graph that has two entities namely sites (nodes) and bonds (edges). We then occupy each site or bond, depending on whether we want to study site or bond percolation, with probability p independent of the state of its neighbors [1]. Broadbent and Hammersley in 1957 first presented the percolation model to understand the motion of gas molecules through the maze of pores in carbon granules filling a gas mask [2]. Since then, the intuitive idea of percolation has been found relevant to so many seemingly disparate systems that its concept has literally percolated across a vast area of science and social science. Examples include flow of fluid in porous media, infiltration in composite materials processing, and the spread of rumors, opinions, and viruses (biological and computer viruses) [3–8].

Besides the simplicity of its definition and the versatility of its application, there exists yet another reason why the percolation model is so popular. In percolation we primarily observe how clusters, a set of contiguous occupied sites, are formed and grown as a function of p, which is the only control parameter. As p value increases from negligibly small, there appears for the first time a cluster that spans across the entire system. In the case of infinite system size, we find a unique threshold value p_c such that there is the probability that the spanning cluster $W(p) = 0$ for $p \leqslant p_c$ and $W(p) = 1$ for $p > p_c$. Interestingly, in such a transition, despite it being geometric in nature, we find many of its aspects reminiscent of a continuous thermal phase transition (CTPT) [9,10]. Thus, percolation serves as a relatively tractable model for the investigation of phase transition and critical phenomena that lie at the heart of the modern development of statistical physics. This is perhaps the most important reason why percolation is still studied extensively even after almost 60 years.

Indeed, for almost every observable quantity in percolation there exists an equivalent counterpart in CTPT. These observables exhibit a power law like their counterpart in CTPT, at least near p_c, which is typically attributed to critical phenomena. For instance, the system size L is like correlation length $L \sim (p - p_c)^{-\nu}$, mean cluster size S is like susceptibility $S \sim (p - p_c)^{-\gamma}$, percolation strength P is like order parameter $P \sim (p - p_c)^{\beta}$, etc. Like a thermal phase transition, the percolation transition, too, can be classified in terms of p_c and by a set of critical exponents β, γ, ν, etc. One of the extraordinary findings in percolation is that the numerical value of its critical exponents depend neither on the detailed nature of the lattice structure nor on the type of percolation, bond, or site. Their values depend only on the dimension of the embedding space of the lattice. It is, therefore, said that percolation on all planar lattices belongs to the same universality class.

Unique universality class has been found true for a variety of periodic and nonperiodic planar lattices having fixed and mixed-valued coordination number, random planar lattices, and their duals, random multifractal lattices, etc. [11–14] (see also Ref. [15], which is the most recent review article). Yet, have we exhausted all the possible lattices to conclude that percolation on all planar lattices belongs to the same universality class? The answer is no. Recently, we have reported that the site percolation on a weighted planar stochastic lattice (WPSL) belongs to a separate and distinct universality class [16]. The WPSL is quite nontrivial as it has mixed properties of both lattice and network or graph [17]. On one hand, unlike networks, it is embedded in the space of dimension $d = 2$, and, on the other hand unlike regular lattice, its coordination number distribution obeys a power law. We have found that the critical exponents for site percolation on the WPSL totally differ from the known values for all other planar lattices studied until now. We, therefore, claim that the random site percolation on the WPSL belongs to a separate and distinct universality class.

In this article, we investigate the bond percolation on the WPSL and present detailed results of its site counterpart in order to see the contrast. One of the goals of the present article is to check if the bond and site percolation on WPSL belong to the same universality class where all the known planar lattices studied to date belong. First, we find the percolation threshold p_c, for both bond and site percolation, using the idea of spanning probability $W(p)$. Second, we attempt to find an estimate for the various critical exponents such as ν, β, and γ using the finite-size scaling hypothesis where precise value of p_c is necessary. Then, we use the idea of data collapse for further fine-tuning of the estimated values for the exponents until we get the best data collapse. Besides critical exponents, we also find the exponent τ that characterizes the cluster size distribution function $n_s(p_c) \sim s^{-\tau}$ and the fractal dimension d_f that characterizes the mass of the spanning cluster $M(p_c) \sim L^{d_f}$. Note that the values of the various critical exponents and the exponents τ, d_f, etc., are not at all independent; rather, they are bound by some scaling relations. We use these scaling relations for a self-consistency check. Our results based on extensive Monte Carlo simulation suggest that both site and bond percolation on WPSL belong to the same universality class and it differs from the one where percolation on all the planar lattices belongs.

The rest of the article is organized as follows. In Sec. II, we discuss the algorithm for the construction of WPSL and some of its key features. In Sec. III, we briefly discuss the Newman-Ziff algorithm as it is the most efficient algorithm for percolation. We also discuss the finite-size scaling and underline its deep connection to the Buckingham Π theorem in Sec. IV. In Sec. V, we present our results about bond and site percolation on the WPSL side by side so we can appreciate the contrast. Finally, we summarize our results in Sec. VI.

II. DESCRIPTION AND CONSTRUCTION OF WPSL

We find it worthwhile to first give a brief description of the construction process of the WPSL. It starts with an initiator which we choose to be a square of unit area. The generator is then defined as the one that divides the initiator (in step one) randomly with uniform probability into four smaller blocks. In step two and thereafter, the generator is applied to only one of the blocks. The question is as follows: How do we pick that block when there are more than one block? The most obvious answer would be to pick preferentially with respect to their areas in the sense that the higher the area, the higher the probability to be picked. For instance, in step one, the generator divides the initiator randomly into four smaller blocks. Let us label their areas a_1, a_2, a_3, and a_4 starting from the top-left corner and moving clockwise. But, of course, this labeling is totally arbitrary and will bear no consequence to the results of any observable quantities. Note that the a_i of the ith block can be regarded as the probability of picking and these probabilities are normalized to $\sum_i a_i = 1$. In step two, one of the four new blocks is picked with probability equal to their respective area, and the generator is applied to divide it randomly into four blocks, resulting in seven blocks or cells in total. Assume that the block 3 with area a_3 is picked and hence this label 3 can be reused. We choose to label the top-left newly created block a_3 and the rest of the blocks are labeled as a_5, a_6, and a_7. At this stage, perhaps giving an exact algorithm for the jth step can help to describe the model better.

(i) Subdivide a unit interval $[0,1]$ into $(3j-2)$ subintervals of size $[0,a_1]$, $[a_1,a_1+a_2]$, $\ldots$, $[\sum_{i=1}^{3j-3} a_i, 1]$, each of which represents the blocks labeled by their areas $a_1, a_2, \ldots, a_{(3j-2)}$, respectively.

(ii) Generate a random number R from the interval $[0,1]$ and find which of the $(3i-2)$ subinterval contains this R. The corresponding block that it represents, say, the pth block with area a_p, is picked.

(iii) Divide the block a_p randomly into four smaller blocks. (To divide it randomly into four blocks we do the following. First, we take note of the length and width of the block a_p and say they are x_p and y_p, respectively. We also take note of the coordinate of the lower-left corner of this block, say, $(x_{\text{low}}, y_{\text{low}})$. Second, we generate two random numbers x_R and y_R from $[0,x_p]$ and $[0,y_p]$, respectively, so the point $(x_{\text{low}}+x_R, y_{\text{low}}+y_R)$ describes the random nucleation of a point through which we draw two mutually perpendicular cut to divide the block a_p into four blocks.)

(iv) Label the four newly created blocks in a clockwise fashion starting from the top-left block, as a_p, $a_{(3j-1)}$, a_{3j}, and $a_{(3j+1)}$, respectively.

(v) Increase time by one unit and repeat the steps (i) through (iv) *ad infinitum*.

The process can also be described as partitioning of a square into ever-smaller mutually exclusive rectangular blocks. It is done by random sequential nucleation of seeds of cracks from which two mutually perpendicular cracks are grown till they are hit or intercepted either by another crack or by the boundary. Note that the higher the area of a block, the higher the probability that the seed will be nucleated on it since seeds are sown at random on the substrate. One advantage of creating WPSL by random sequential partitioning of a square helps in defining each step of the division process as one time unit. The number of blocks N at time t therefore is $N = 1 + 3t$ and hence it grows, albeit the sum of the areas of all the blocks is always equal to the size of the initiator. It implies that the number of blocks N increases with time t at the expense of the size of the blocks. Thus, if we want to compare the value of an observable quantity O for different size of WPSL, then we need to magnify the lattice by $3t$ provided O depends on the block size of WPSL.

III. VARIOUS PROPERTIES OF WPSL

The snapshot of the WPSL shown in Fig. 1 clearly gives an impression that it is seemingly complex, manifestly intricate, and inextricably intertwined. Such a disordered lattice, that emerges through evolution, can only be useful if the snapshots taken at different late stages are similar. To this end, we have recently shown that the area size distribution of the blocks of WPSL obeys dynamic scaling,

$$c(a,t) \sim t^{\theta} \phi(a/t^{z}), \tag{1}$$

where we found $\theta = 2$ and $z = -1$ [18]. We have proved it using the idea of data collapse (see Fig. 2). Note that the data collapse means that the numerical values of the dimensional quantities $c(a,t)$ and a are distinct for different time *vis-à-vis* different sizes of WPSL. However, the corresponding

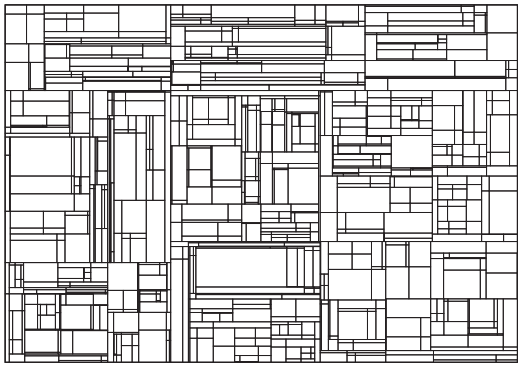

FIG. 1. A snapshot of the weighted stochastic lattice.

dimensionless quantity $c(a,t)/t^{\theta}$ at different times for a fixed value of dimensionless quantity a/t^{z} coincides. It implies that the snapshots of the lattice at different times are similar [19]. Furthermore, instead of characterizing the blocks by areas, they can also be characterized by their length x and width y. We can then write the rate equation for the corresponding distribution function $c(x,y;t)$ as

$$\frac{\partial c(x,y;t)}{\partial t} = -a(x,y)c(x,y;t) + 4\int_x^{\infty}\int_y^{\infty} dx_1 dy_1 \times c(x_1,y_1;t)F(x,x_1-x,y,y_1-y), \quad (2)$$

where

$$a(x,y) = \int_0^x \int_0^y dx_1 dy_1 F(x_1,x-x_1,y_1,y-y_1). \quad (3)$$

Here kernel $F(x_1,x_2,y_1,y_2)$ determines the rules and the rate at which the block of sides (x_1+x_2) and (y_1+y_2) is divided into four smaller blocks whose sides are (x_1,y_1), (x_2,y_1), (x_1,y_2), and (x_2,y_2) (see for detailed description Refs. [20–22]). The first term of the right-hand side of Eq. (2) represents the loss due to breakup of blocks having sides x and y and the second term represents the gain of blocks of sides x and y due to breakup of blocks having sides $x_1 > x$ and $y_1 > y$. The factor 4 on the second term is due to the fact that at each time step the process gives birth to four smaller blocks.

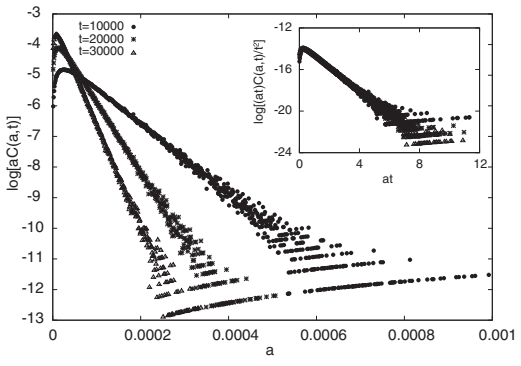

FIG. 2. Plots of $\log[aC(a,t)]$ are shown as function of a for three different times. In the inset we plot $\log(atC(a,t)$ versus at and find that all the distinct plots collapse into one universal curve, revealing that $C(a,t) \sim (at)^{-1}e^{-at}$.

We must choose the following fragmentation kernel in order to describe the construction of WPSL:

$$F(x_1,x_2,y_1,y_2) = 1. \quad (4)$$

The appropriate rate equation for $c(x,y,t)$ then is

$$\frac{\partial c(x,y;t)}{\partial t} = -xyc(x,y;t) + 4\int_x^{\infty}\int_y^{\infty} c(x_1,y_1;t)dx_1 dy_1. \quad (5)$$

Solving it to find an exact solution for $c(x,y;t)$ can be a formidable task. We instead focus on the 2-tuple Mellin transform $M(m,n,t)$ of $c(x,y,t)$ itself defined as

$$M(m,n;t) = \int_0^{\infty}\int_0^{\infty} x^{m-1}y^{n-1}c(x,y;t)dxdy, \quad (6)$$

whose discrete counterpart is $\sum_i^N x_i^{m-1}y_i^{n-1}$. Incorporating it into Eq. (5), we find

$$\frac{dM(m,n;t)}{dt} = \left(\frac{4}{mn}-1\right)M(m+1,n+1;t). \quad (7)$$

A surprising feature of the above equation is that it implies the existence of infinitely many nontrivial conservation laws: $M(m,4/m;t) \ \ \forall\ m$ independent of time. To solve Eq. (7) we iterate it over and over again to get all the derivatives of $M(m,n;t)$ and then, according to Charlesby's method, we substitute those derivatives into the Taylor series expansion of $M(m,n;t)$ about $t=0$. This gives a solution for $M(m,n;t)$ in terms of the generalized hypergeometric function [23]

$$M(m,n;t) = {}_2F_2(a_+,a_-;m,n;-t), \quad (8)$$

which takes the following simple form in the long-time limit:

$$M(m,n,t) \sim t^{-a_-}, \quad (9)$$

where

$$a_- = \left[\frac{m+n}{2} - \sqrt{\left(\frac{m-n}{2}\right)^2+4}\right]. \quad (10)$$

The above solution can provide everything that we want to learn about WPSL.

Note that the fraction of the measure, conserved quantity $\sum_i^N x_i^{(4/m)-1}y_i^{m-1}$, that the ith block contains is $x_i^{(4/m)-1}y_i^{m-1}$. This quantity can be regarded as the probability p_i and hence its qth moment is

$$Z_q = \sum_i p_i^q \sim \sum_i^N x_i^{(4/m-1)q}y_i^{(m-1)q} = \sum_i^N x_i^{((4/m-1)q+1)-1}y_i^{((m-1)q+1)-1}. \quad (11)$$

Comparing it with the solution for the discrete counterpart of $M(m,n;t)$ yields

$$Z_q = M[(4/m-1)q+1,(m-1)q+1;t]. \quad (12)$$

Using Eq. (9) we can immediately write the asymptotic solution for Z_q as

$$Z_q(t) \sim t^{\{\sqrt{(4/m-m)^2q^2+16}-(4/m+m-2)q+2)\}/2}. \quad (13)$$

We can now measure Z_q in the unit of a suitable yardstick:

$$\delta(t) = \sqrt{\frac{M(2,2;t)}{M(1,1;t)}} \sim t^{-1/2}, \tag{14}$$

which is the square root of the mean area of the blocks at time t. Eliminating time t in favor of δ, we find that Z_q decays following a power law,

$$Z_q(\delta) \sim \delta^{-\tau(q,m)}, \tag{15}$$

where the mass exponent

$$\tau(q,m) = \sqrt{(4/m-m)^2q^2+16} - [(4/m+m-2)q+2]. \tag{16}$$

The mass exponent $\tau(q,m)$ must satisfy two conditions regardless of the value of n: (i) $\tau(0,n) = d$ is the dimension of the support which is equal to 2 in this case and (ii) $\tau(1,m) = 0$ as required by the normalization condition $\sum_i p_i = 1$ [24]. The Legendre transform of $\tau(q,m)$ is

$$\tau(q) = -\alpha q + f(\alpha), \tag{17}$$

where the derivative

$$\alpha = -\frac{d\tau(q,m)}{dq} \tag{18}$$

is now the independent variable instead of q. It implies that for every m value there exists a spectrum of spatially intertwined fractal dimensions

$$f(\alpha(q,m)) = \frac{16}{\sqrt{\left(\frac{4}{m}-m\right)^2q^2+16}} - 2, \tag{19}$$

which are needed to characterize the WPSL except for $m = 2$. Note that the $f(\alpha,m)$ spectrum is always concave in character, as shown in Fig. 3. Besides, the maximum value of $f(\alpha,m)$ always occurs at $q = 0$, which corresponds to the dimension of the embedding space. The dimension of the embedding space of the WPSL is equal to 2. Besides, we find that there exists a spectrum of multifractal spectra depending on the value of m and hence we regard WPSL as a multifractal planar lattice.

The snapshot of WPSL shown in Fig. 1 clearly reveals that it is a planar cellular structure whose cells or blocks have great many different numbers of neighbors. To find the nature

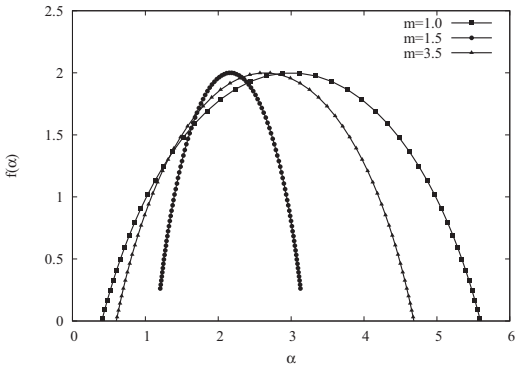

FIG. 3. The $f(\alpha)$ spectrum for $m = 1.0, 1.5, 3.5$.

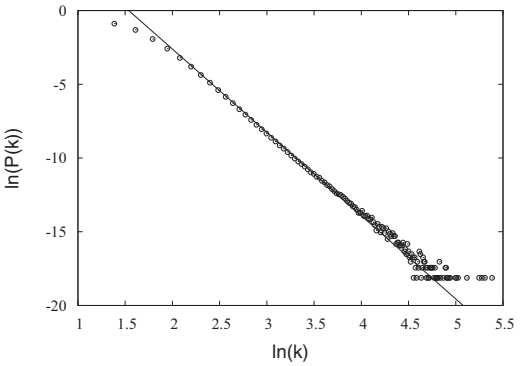

FIG. 4. Coordination number distribution of WPSL (or degree distribution function of its dual) $P(k)$ is the fraction of the total blocks which has coordination number k. The slope of the straight line is $\theta = 5.56$, revealing that $P(k) \sim k^{-\theta}$. The plot represents the ensemble average of 500 independent realizations of lattice size $t = 50\,000$.

of its coordination number distribution, we look at its dual, obtained by replacing each block with a node at its center and common border between blocks with an edge or link joining the two vertices, and find that it becomes a network. We know that each node in the network can be best characterized by its degree k. It is defined as the number of links by which a given node is connected to other nodes. One of the most important observables in the network theory is to find how the degrees of its nodes are distributed. That is equivalent to finding the fraction of the total nodes which has degree k which can also describe the probability $P(k)$ that a node picked at random has a degree k. Note that the coordination number distribution in the WPSL and the degree distribution of its dual are identical. In Fig. 4 we plot $\ln(P)k)$ vs $\ln(k)$ and find a straight line, at least near the tail, with slope equal to 5.56, revealing that $P(k)$ follows a power law $P(k) \sim k^{-\theta}$ with $\theta = 5.56$ [17]. Note also that the plot $\ln[P(k)]$ vs $\ln(k)$ has a characteristic fat tail, which is the signature of the scarce data points along the tail of the $P(k)$ versus k which are actually the hubs. We thus can say that the coordination number distribution of the WPSL is scale free. This is in sharp contrast to the coordination number distribution in the Voronoi diagram where it is also random but its distribution is peaked around the mean [25]. In the Voronoi diagram, it is almost impossible to find cells or blocks which have significantly higher or fewer neighbors than the mean coordination number. That is, here the mean describes the characteristic scale. Such a characteristic scale is absent in the WPSL since the distribution function follows a power law. The power-law coordination number distribution also means that the majority of the blocks in the WPSL are very poor in coordination number and there are few cells or blocks which have significantly high number of nearest neighbors. We also find the mean nearest-neighbors number of the WPSL. In the case of a site, it is 5.333 and in the case of a bond it is 10.01. However, due to the power-law nature of the coordination number distribution, the standard deviation of their respective quantities are quite high. For instance, we find the standard deviations for site and bond to be 1.88 and 4.0, respectively.

IV. NEWMAN-ZIFF ALGORITHM

In standard algorithms, such as the Hoshen-Kopelman (HK), one must create an entire new state for every given value of occupation probability p in every independent realization. Investigation of the various observables using such traditional algorithms are highly expensive in terms of computational time and accuracy of finding various observable quantities. In 2000, Newman and Ziff (NZ) proposed an algorithm which is highly efficient in both accounts [26]. The efficiency of the NZ algorithm lies in the fact that one creates a new state with $n+1$ occupied sites or bonds from the immediate previous state with n occupied sites or bonds simply by occupying one extra randomly chosen site or bond. It is based on the intuitive idea of random sequential adsorption of sites or bonds on a given lattice or graph.

The algorithm is trivially simple. One starts with an empty lattice. Then, at each step, an empty site or bond is chosen at random and then is occupied if empty; otherwise, the attempt is discarded. However, in order to further reduce the computation time, we first decide on an order in which the sites or bonds will be occupied. That is, we wish to choose a random permutation of the bonds or sites. This is done by creating a list of all the bonds in any convenient order. Positions in this list are numbered from $1,2,3,\ldots,M$. Choose a number j at random with uniform probability in the range $i \leqslant j \leqslant M$. Then we use any standard textbook algorithm to randomize the number $i = 1$ to M and put them in the new order in which they will be occupied. Having chosen an order of all the sites, we start occupying them in that order. The first site or bond to be occupied will definitely form a cluster of size one. The second, third, fourth, etc., are also highly likely to form clusters of size one. However, the likelihood of forming clusters of size one will decrease with the number of occupied sites since some sites, when occupied, will become contiguous occupied sites, thus making clusters of size more than one.

The formation of clusters and the statistics of their sizes are the key to the study of percolation theory. In the case of the NZ algorithm, we measure an observable, say, O, for fixed numbers of occupied sites (or bonds) and obtain data for O as a function of occupation number n. This is in sharp contrast with the HK algorithm, where the number of sites being occupied at a given p is random and differs at every independent realization. However, if the system size is large enough, then the mean occupation number will almost equal pN, where N represents the system size. The weight factor of obtaining different n for a given p are not the same. The exact weighting factor of there being exactly n occupied sites on the lattice for a given p is given by a binomial distribution,

$$C(n,N,p) = \binom{N}{n} p^n (1-p)^{N-n}. \tag{20}$$

The binomial coefficient $\binom{N}{n}$ represents the number of possible configurations of n occupied sites and $N-n$ empty sites. Using this and the data for the observable O for all values of n, we can find O for any value of p by the following relation:

$$O(p) = \sum_{n=1}^{N} \binom{N}{n} p^n (1-p)^{N-n} O_n. \tag{21}$$

It is interesting to note that the ensemble of states with exactly n occupied sites or bonds obtained according to the NZ algorithm can be referred to as a *microcanonical percolation ensemble*, where the number n is the equivalent counterpart of the energy E in thermal statistical mechanics. On the other hand, if we keep p fixed instead of n we can regard it as the canonical ensemble.

V. SITE AND BOND PERCOLATION ON WPSL

What is site and bond in WPSL? Before answering this question, we find it worth discussing first what they are in the context of conventional lattices. For instance, we can regard a square lattice as a grid or mesh. Each cell of the grid has four sides and each side is a common border of two cells only. In the case of a square grid, we can thus regard each cell as a site since it contains exactly one lattice point. Equivalently, we could also regard the vertices of each cell as sites. However, in the present context, we stick to the former definition. The dual of the square grid, obtained by replacing the center of each cell by a node and the common border between neighboring cells by a link connecting the two nodes, is also a square lattice and hence it is called self-dual. Here, the links of the dual are like the bonds of the square lattice. Following the same argument, we regard the blocks of the WPSL as its sites and not the vertices of the lines that tessellated the initiator. To define a bond, we first find its dual. It is obtained by replacing the center of each block by a node and the common border between two neighboring blocks by a link connecting the corresponding nodes. We regard these links as the bonds of the WPSL. Using these ideas, we first performed site and bond percolation on the square lattice and reproduced all the known results and then we applied them to the WPSL.

In the case of bond percolation, the lattice consists initially of N blocks and hence the system has exactly N number of clusters of size one since the center of each block represents a site. Thereafter, each time we occupy a bond, a cluster at least of size two or more is formed. In the case of site percolation, each time we occupy a block, the size of the cluster may vary as we measure it by the area of contiguous occupied blocks, not by the number of occupied sites. Initially all the blocks are empty and there is no cluster. For a regular lattice, like a square lattice, the L^2 sites have $2L(L-1)$ and $2L^2$, bonds with open and periodic boundary conditions, respectively. Now WPSL, being a disordered lattice, cannot have such an exact relation. We still find that the number of bonds or sites when we take the average over an ensemble of independent realizations follows a relation valid for all sizes of the lattice. For instance, for the lattice at time t there are exactly $3t+1$ sites and, on average, there are $8t$ bonds with the periodic boundary condition. Thus, the mean coordination number is equal to $16t/3t \sim 5.33$, which is higher than that of the square lattice. We know that the percolation threshold p_c depends on the coordination number of the lattice, and the higher the mean coordination number of a lattice, the smaller the value of p_c. In the case of a square lattice, for instance, each site has exactly four nearest neighbors and each bond has six, and hence the p_c of the site percolation is higher than that of the bond. On the other hand, the mean coordination number of the site

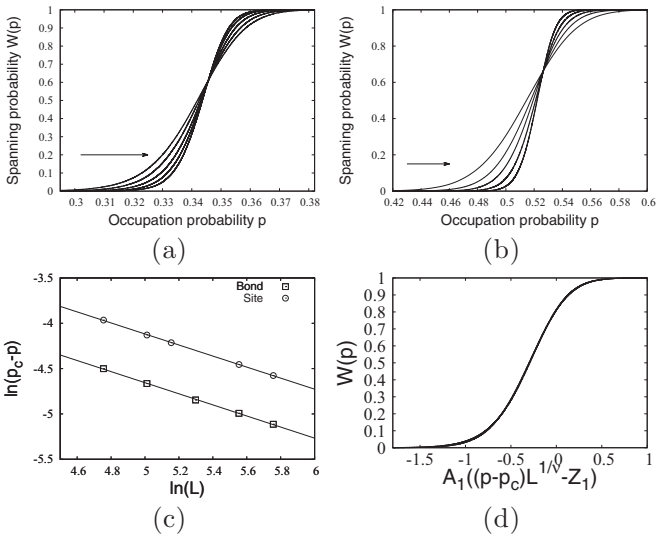

FIG. 5. Spanning probability $W(p,L)$ vs p in WPSL for (a) bond and (b) site percolation. The simulation result of the percolation threshold is $p_c = 0.3457$ for bond and 0.5265 for site. In (c) we plot $\log(p - p_c)$ vs $\log L$ for both bond and site. The two lines have slopes $1/\nu = 0.6117 \pm 0.0074$ and 0.6135 ± 0.0038 for bond and site, respectively. In (d) we plot dimensionless quantities W vs $A_1[(p - p_c)L^{1/\nu} - Z_1]$ and we find an excellent data collapse of all the distinct plots in (a) and (b) if we use $Z_1 = 0.194$ and $A_1 = 1$ for bond and $A_1 = 0.798$ for site.

in the WPSL is 5.33 and that of triangular lattice 6 and the corresponding p_c values are 0.5265 and 0.5, respectively.

A. Spanning probability $W(p)$

The spanning probability $W(p)$ for both the bond and site describe the likelihood of finding a cluster that spans across the entire system either horizontally or vertically at the occupation probability p. To find how $W(p)$ behaves with the control parameter p, we perform many, say, M, independent realizations under the same identical conditions. In each realization for a given finite system size, we take the record of the p_c value at which the spanning cluster appears for the first time. To find a regularity or a pattern among all the M numbers of p_c values recorded, one usually looks at the relative frequency of occurrence within a class or width Δp. To find $W(p)$, we can process the data containing M number of p_c values to plot a histogram displaying the normalized relative frequency as a function of class of width Δp chosen as per convenience. In Figs. 5(a) and 5(b) we show a set of plots of $W(p)$ for bond and site percolation, respectively, as a function of p where distinct curves are for different system sizes $L = \sqrt{N}$. One of the significant features of such plots is that they all meet at one particular p value regardless of the value of L. It means that even if we had data for an infinite system, the resulting plot would still meet at the same point, revealing that it must have a special significance and the significance is that it is the threshold probability p_c. Note that finding the p_c value for different lattices is one of the central problems in percolation theory [27,28]. In the case of a bond, we find $p_c = 0.3457$, which is far less than its site counterpart, $p_c = 0.526846$. We know that the higher the coordination number, the smaller the p_c. For instance, the coordination numbers (the number of nearest neighbors) of a site and bond of the triangular lattice are 6 and 10 and their p_c values are 0.5 and 0.347296355, respectively. On the other hand, the coordination number of site of the WPSL is not fixed but rather follows a power law. Yet, we find that its mean coordination number 5.33 is slightly less than the mean coordination of the triangular lattice. We therefore find the p_c of the former is slightly higher than that of its triangular counterpart. The same is true for bond type. Note that the nearest number of bonds of a bond in the triangular lattice and that of the WPSL are almost the same, albeit the latter is slightly higher and hence the corresponding p_c of the WPSL is slightly lower than that of its triangular counterpart.

The second most significant feature of the $W(p)$ vs p plot is the direction of shift of the curves on either side of p_c as the system size L increases. This shift with L clearly reveals that all the data points, i.e., the p values, are marching towards p_c. We can quantify the extent at which they are marching by measuring the magnitude of the difference $(p_c - p)$ for different L. That is, we can draw a horizontal line at a given value of W, preferably at the position where this difference is the most, and take records of the difference $p_c - p$ as a function of system size L. Plotting the resulting data after taking log of both the variables or in the logarithmic scale we find a straight line whose slope gives an estimate of the inverse of $1/\nu = 0.6135 \pm 0.0038$ since Fig. 5(c) suggests

$$p_c - p \sim L^{-\frac{1}{\nu}}. \tag{22}$$

It implies that in the limit $L \to \infty$ all the p takes the value p_c, revealing that $W(p)$ will ultimately become a step function so $W(p) = 0$ for $p \leqslant p_c$ and $W(p) = 1$ for $p > p_c$. We can use Eq. (22) to define a dimensionless quantity $(p_c - p)L^{\frac{1}{\nu}}$. Now, if we plot $W(p)$ vs $(p_c - p)L^{\frac{1}{\nu}}$, we find that all the distinct curves for bond in Fig. 5(a) collapse into one as does that for the site in Fig. 5(b) sharing the same ν value. However, we know that the universality means not only that they share the same exponents but also that they have the same scaling functions which may differ at best by some constant factor and/or by a trivial shift. In general, scaling functions for bond and site collapse if one plot $A_2 W L^{-a/\nu}$ vs $A_1(p - p_c)L^{1/\nu}$ where A_1 and A_2 are known as matric factors and we already know that $a = 0$ for spanning probability. To check it, we first plot W vs $x = (p - p_c)L^{1/\nu}$ for both bond and site on the same graph. We find that height of the two scaling functions are the same, which implies that $A_2 = 1$ for both bond and site. We also observe that, unlike all other planar lattices, the two scaling functions do not cross at $x = 0$ but rather they cross at $x = 0.194$. It implies that we have to subtract $Z_1 = 0.194$ from x of data for both bond and site. Furthermore, following the procedure described in Ref. [29], we find $A_1 = 1$ for bond and $A_1 = 0.798$ for site. Now plotting W vs $A_1(x - Z_1)$ gives a perfect data collapse as shown in Fig. 5(d). It implies that not only is the $1/\nu$ value independent of the type of percolation but also that they share the same form for the scaling function.

B. Percolation probability P

Consider that we pick a site at random and ask: How likely is that that site to belongs to the spanning cluster? For a finite

system size, it may not belong to the spanning cluster even if p is larger than the percolation threshold p_c. We can therefore quantify the strength of the spanning cluster by percolation probability P, which describes how likely a site being picked at random is to belong to the spanning cluster. The quantity P is defined as the ratio of the size of the spanning cluster s_∞ to the size of the lattice N, i.e.,

$$P = \frac{\text{Number of sites in the spanning cluster}}{\text{Total number of sites in the lattice}}. \quad (23)$$

Sometimes, percolation probability is also defined as the probability that an occupied site belongs to the spanning cluster. It can be obtained if we replace the denominator N of Eq. (23) by total number of occupied sites. We, however, will consider the former definition. There exists yet another definition where we can use the size of the largest cluster instead of the spanning cluster. Note that all these definitions behave in the same fashion like order parameter. That is, in the limit $L \to \infty$, $P = 0$ for $p \leqslant p_c$ and it rises from $P = 0$ at p_c to $P = 1$ continuously and monotonically like $P \sim (p - p_c)^\beta$. Such behavior is reminiscent of order parameter like magnetization m in the ferromagnetic transition, and hence P is regarded as the order parameter in percolation theory. The critical exponent β value is known to depend only on the dimension of the lattice and independent of the type of percolation. Through the site percolation on WPSL, we already reported that the β value for WPSL, which is a planar lattice, differs from the value for all the known planar lattices whose dimension of the embedding space $d = 2$. We shall now check if the β value for the bond percolation is the same as for the site percolation.

It is important to note that in the case of site percolation, we occupy its blocks or cells which are of different sizes. We therefore quantify the size of the spanning cluster by its area and not by the number of sites or blocks in the spanning cluster. Note that for bond percolation on WPSL we use the dual of the WPSL and not the lattice itself. The dual of the WPSL is obtained by replacing each block of the WPSL by a node or vertex at its center and each common border between blocks by a bond connecting the nodes at the center of corresponding blocks. We then occupy these links and measure the size of the cluster by the number of nodes or vertices that the cluster contains. Below we shall see the impact of this difference in their behavior, if at all. In Figs. 6(a) and 6(b), we plot percolation probability P as a function of p for bond and site, respectively. Looking at the plots, one may think that all the plots for different L meet at a single unique point like it does for the $W(p)$ vs p plot. However, if one zooms in, then it becomes apparent that this is not so and hence the p_c value from this plot will not be as satisfactory as it is from $W(p)$ vs p plot. We also find that $P(p)$ is not strictly equal to zero at $p < p_c$; instead, there is always a nonzero chance of finding a spanning cluster even at $p < p_c$ as long as the system size L is finite. However, the plots of P vs p for different system sizes L reveal that the chances of getting a spanning cluster at $p < p_c$ diminishes with increasing L. There is also a lateral shift of the P value to the left for $p > p_c$ but the extent of this shift $p - p_c$ decreases to such a degree that it never diminishes. On the other hand, the extent of the shift $p - p_c$ to the right for $p < p_c$ diminishes to zero following Eq. (22). We shall now

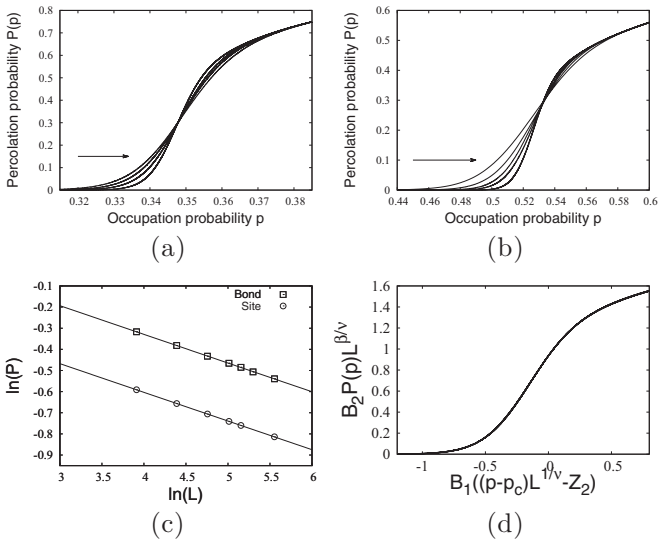

FIG. 6. Percolation probability $P(p,L)$ vs p for (a) bond and (b) site percolation. In (c) we plot log P vs log L using data for fixed value of $(p - p_c)L^{1/\nu}$ and find almost parallel lines with slopes $\beta/\nu = 0.1356 \pm 0.0005$ and 0.1357 ± 0.0002 for bond and site, respectively. In (d) we plot $B_2 P L^{\beta/\nu}$ vs $B_1((p - p_c)L^{1/\nu} - Z_2)$ and find excellent data collapse of all the distinct plots of (a) and (b) if we use $B_1 = 1$, $B_2 = 1$, and $Z_2 = 0.225$ for bond and use $B_1 = 0.69$, $B_2 = 1.443$, and $Z_2 = 0.225$ for site.

check if P above p_c grows like $P \sim (p - p_c)^\beta$. If it does, then we shall find the value of the critical exponent β and compare it with that of its site counterpart.

To show that the percolation probability behaves like $P \sim (p - p_c)^\beta$ and to find the exponent β for infinite system size L, we use the idea of finite-size scaling. We first plot $P(p)$ vs $(p - p_c)L^{1/\nu}$ and find that, unlike $W(p)$ vs $(p - p_c)L^{1/\nu}$, it does not collapse. Instead, we find that for a given value of $(p - p_c)L^{1/\nu}$ the P value decreases with lattice size L. It means percolation probability is not a dimensionless quantity and hence we assume that

$$P \sim L^{-a} \quad (24)$$

and choose $a = \beta/\nu$ for later convenience. To find the value of β/ν, we measure the heights at a given value of $(p - p_c)L^{1/\nu}$ for different L and plot them in the log-log scale. We find straight lines for both bond and site [see Fig. 6(c)] with slopes $\beta/\nu = 0.1356 \pm 0.0005$ for bond and 0.1357 ± 0.0002 for site, revealing that they are almost parallel. It implies that if we now plot $P L^{\beta/\nu}$ vs $(p - p_c)L^{1/\nu}$, then all the distinct plots of P vs p for site and bond should collapse, at least separately, into a single universal curve. However, the respective data-collapse curves for bond and site should also collapse if we plot $B_2 P L^{\beta\beta/\nu}$ vs $B_1((p - p_c)L^{1/\nu} - Z_2)$ with suitable value of B_1, B_2 and Z_2 for bond and site percolation. To find these constants, we first plot $P L^{\beta/\nu}$ vs $(p - p_c)L^{1/\nu}$ for bond and site on the same graph. We observe that, like in the square lattice, the peak heights for bond and site differ, which implies that B_2 for bond and site are not equal and we find $B_2 = 1$ for bond and for site $B_2 = 1.443$. We then plot $B_2 P L^{\beta/\nu}$ vs x and find that, unlike the square lattice, they do not cross at $x = 0$ but rather at 0.225, which implies that $Z_2 = 0.225$. Following the

procedures in Ref. [29] we find $B_1 = 1$ for bond and $B_1 = 0.69$ for site. Plotting now $B_2 P L^{-\beta/\nu}$ vs $B_1(x - Z_2)$, we find that the scaling functions for site and bond both collapse superbly onto each other, which is shown Fig. 6(d). This again implies that percolation probability P exhibits finite-size scaling,

$$P(p_c - p, L) \sim L^{-\beta/\nu}\phi[(p - p_c)L^{1/\nu}]. \tag{25}$$

Now using Eq. (24) in Eq. (25) to eliminate L in favor of $p - p_c$, we get

$$P \sim (p - p_c)^{\beta}, \tag{26}$$

where $\beta \sim 0.222$ independent of site or bond percolation and it significantly differs from the corresponding values for all known planar lattices.

C. Cluster size distribution and their mean

The cluster size distribution function $n_s(p)$ plays a central role in the description of percolation theory. It is defined as the number of clusters of size s per site in the lattice. The quantity $sn_s(p)$ then is the probability that an arbitrary site belongs to a cluster of size s. On the other hand, the quantity $\sum_{s=1} sn_s$ is the probability that an arbitrary site belongs to a cluster of any size which is in fact equal to p. One can then define the probability that an occupied site chosen at random belongs to a cluster of size exactly equal to s as

$$f_s = \frac{sn_s(p)}{\sum_{s=1} sn_s}. \tag{27}$$

The mean cluster size $S(p)$ therefore is given by

$$S(p) = \sum_s sf_s = \frac{\sum_s s^2 n_s}{\sum_s sn_s}, \tag{28}$$

where the sum is over the finite clusters only, i.e., the spanning cluster is excluded from the enumeration of S. The definition of the mean cluster size S, however, does not have information about the geometric structure of the clusters like their compactness and spatial extent. In the case of site percolation on WPSL, the mean cluster size cannot be quantified by the number of sites but the amount of area. This is because the typical or mean size of each block or cell of the WPSL decreases like $(1 + 3t)^{-1}$ with the increase in the lattice size which we quantify by number of blocks $N = 1 + 3t$. We thus need to blow up the lattice by a factor of $1 + 3t$ in order to compensate for the decreasing block size with increasing block number N. Thus, we define the mean cluster size for site percolation on WPSL as

$$S = \frac{1}{p}\sum_s s^2 n_s 3t. \tag{29}$$

In the case of bond percolation, however, we do not need to multiply by the factor $3t$ as the cluster size here is measured by the number of nodes or vertices it contains, not by the area.

In Figs. 7(a) and 7(b) we show the plots of the mean cluster size $S(p)$, for both bond and site percolation, as a function of p for different lattice sizes L. We observe that in either case, there are two main effects as we increase the lattice size. First, we see that the mean cluster size increases as we increase the occupation probability until p approaches p_c and the peak

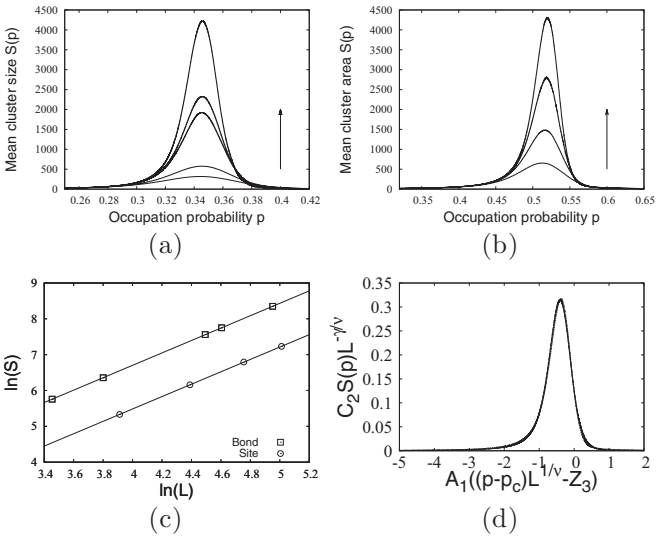

FIG. 7. The mean cluster size $S(p, L)$ vs p for (a) bond and (b) site percolation as a function of system size. In (c) we plot log S vs log L using the size of S for fixed value of $(p - p_c)L^{1/\nu}$ and find almost parallel lines with slopes $\gamma/\nu = 1.7315 \pm -0.0019$ and 1.7280 ± 0.0019 for bond and site, respectively. In (d) we plot $C_2 SL^{-\gamma/\nu}$ vs $C_1[(p - p_c)L^{1/\nu} - Z_3]$ and find that all distinct plots of (a) and (b) collapse into one universal curve if we use $C_1 = 1, C_2 = 1, Z_3 = 0.40$ for bond and $C_1 = 0.625$, $C_2 = 1.10$, $Z_3 = 0.40$ for site.

height grows profoundly with L in the vicinity of p_c. Second, there is a slight shift in the peak towards the p_c value as we increase L. The extent of the shift is again given by Eq. (22). To bring the peak height to meet at the same point, we first plot S as a function of dimensionless quantity $(p_c - p)L^{1/\nu}$. We then measure the peak height for a fixed value of $(p_c - p)L^{1/\nu}$ but for different L. Plotting these peak heights as a function of L in the log - log scale gives straight lines for site and bond percolation (see the inset of Fig. 7(c). It implies that

$$S \sim L^{\theta}, \tag{30}$$

where, like before, we again choose $\theta = \gamma/\nu$ for future convenience and find that $\gamma/\nu = 1.7315 \pm 0.0019$ for bond and 1.7280 ± 0.0019 for site. The two values are so close that they can be well approximated to be the same. Plotting now the same data of Figs. 7(a) and 7(b) by measuring the mean cluster size S in the unit of L^{θ} and $(p_c - p)$ in the unit of $L^{-1/\nu}$, respectively, we find that all the distinct plots of S vs p collapse superbly into universal curves. However, like for the percolation probability P, here, too, the scaling functions for bond and site do not collapse if we plot $SL^{-\gamma/\nu}$ vs $(p_c - p)L^{1/\nu}$ since they differ by some constant factors. Indeed, we show in Fig. 7(d) that if we plot $C_2 SL^{-\gamma/\nu}$ vs $C_1((p - p_c)L^{1/\nu} - Z_3)$ and choose $C_1 = C_2 = 1$ and $Z_3 = 0.40$ for bond while $C_1 = 0.625$, $C_2 = 1.10$, and $Z_3 = 0.40$ for site and find all the distinct plots Figs. 7(a) and 7(b) collapse superbly into one universal curve. It again implies that the mean cluster size, too, for both bond and site, exhibits finite-size scaling,

$$S \sim L^{\gamma/\nu}\phi[(p_c - p)L^{1/\nu}], \tag{31}$$

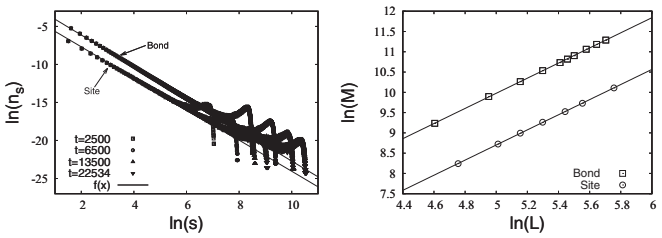

FIG. 8. We plot (a) the cluster size distribution function $\log[n_s(p_c)]$ vs $\log s$ for different sizes of the WPSL and find almost parallel lines with slopes 2.07252 and 2.0728 for bond and site percolation, respectively. (b) The mass of the spanning cluster M is shown as a function of system size L. The two lines with slopes $d_f = 1.8637 \pm 0.0224$ and 1.8643 ± 0.0014 for bond and site, respectively, once again reveal that the fractal dimension of the spanning cluster is independent of the type of percolation.

sharing the same critical exponents. Eliminating L from Eq. (22) in favor of $(p_c - p)$ using $(p_c - p) \sim L^{-1/\nu}$, we find that the mean cluster diverges

$$S \sim (p_c - p)^{-\gamma}, \tag{32}$$

where $\gamma = 2.825$ for both site and bond percolation. This value differs significantly from the known value $\gamma = 2.389$ for all the regular planar lattices.

It is well known that the cluster size distribution $n_s(p)$ obeys

$$n_s(p) \sim s^{-\tau}\phi[(p - p_c)^{1/\sigma}s], \tag{33}$$

and hence at $p = p_c$ it is

$$n_s(p_c) \sim s^{-\tau}, \tag{34}$$

where τ is called the Fisher exponent. We can obtain the value of τ by plotting the cluster area distribution function $n_s(p)$ at p_c. In Fig. 8(a) we plot $\ln[n_s(p_c)]$ vs $\ln(s)$, for both site and bond, and find two parallel lines except near the tail where there is a hump due to the finite-size effect. However, we also observe that as the lattice size L increases, the extent up to which we get a straight line increases, too. This implies that if the size L were infinitely large, then we would have a perfect straight line obeying Eq. (34). The slopes of the lines are $\tau = 2.0725$ for bond and $\tau = 2.0728$ for site. It implies that the exponent τ is almost the same $\tau \sim 2.072$ for both site and bond percolation on WPSL and its value differs from the value for all known planar lattices $\tau = 2.0549$.

Let $M(L)$ denote the mass or size of the percolating cluster at p_c of lattice of linear size L. Now we check the geometric nature of this spanning cluster. First, if the cluster is a Euclidean object, then its mass $M(L)$ would grow as $M(L) \sim L^d$ with $d = 2$ since the dimension of the embedding space of the WPSL is $d = 2$. Now, a litmus test of whether the spanning cluster is a fractal would be to check if it obeys the same mass-length relation but with an exponent $d = d_f < 2$. To find this out, we plot the size or mass of the spanning cluster M as a function of lattice size L in the log-log scale as shown in Fig. 8(b). Indeed, we find a straight line with slope $d_f = 1.8643 \pm 0.0014$ for site and $d_f = 1.8637 \pm -0.0224$ for bond which are almost the same but significantly differ from the one for all known regular planar lattices $d_f = 1.895$. It may appear that the difference between the d_f for WPSL and that for regular planar lattices is not much but it is important to remember that even a small difference in fractal dimension has a huge effect on their degree of ramification. It is well known that the numerical values of the various exponents β, γ, τ, d_f, etc., depend only on the dimension of the lattice and independent of the nature of structure of the lattice and the type of percolation. However, their values are bound by some scaling and hyperscaling relations such as $\tau = 3 - \gamma\sigma$, $\tau = 1 + d/d_f$, $\beta = \nu(d - d_f)$, $\gamma = \nu(2d_f - d)$, etc. We can use these relations for a consistency check of our results. To this end, we find that our estimates satisfy these relations to a good extent.

VI. SUMMARY AND DISCUSSION

In this article, we have studied both bond and site percolation on WPSL using extensive Monte Carlo simulations. We thought it would be important to know some key features of the WPSL so one can understand why it is so special and unique. We therefore have first briefly discussed its construction process and then its various properties. Some of its key features are as follows. First, the dynamics of its growth is governed by infinitely many conservation laws. Second, its area size distribution function obeys dynamic scaling. Third, each of the infinitely many conservation laws, except conservation of total area, gives rise to multifractal spectrum and hence WPSL is a multifractal. Fourth, its coordination number distribution function follows a power law. Finally, note that it has a mixture of properties of both lattice and graph. On one hand, like a lattice, it is embedded in a space of dimension $D = 2$; on the other hand, its coordination number distribution follows a power law.

The primary goal of this article is to study bond percolation on the WPSL and check if it belongs to the same universality class where its site counterpart belongs [16]. To this end, we have first obtained the percolation threshold $p_c = 0.3457$ for a bond, which is less than the $p_c = 0.5265$ of the site percolation, as expected. We also studied numerically the spanning probability $W(p)$, the percolation strength $P(p)$, and the mean cluster size $S(p)$ using the NZ algorithm. The resulting data are then used in the convolution equation to obtain data that correspond to a canonical ensemble. Then, with the help of a comprehensive finite-size scaling theory, we obtained the various exponents ν,β, γ, τ, and d_f for both bond and site percolation on WPSL and confirm that the respective exponents for site and bond are equal (see Table I for a detailed comparison). Note that in all cases we found excellent data collapse for site and bond, sharing the same

TABLE I. The characteristic exponents for site and bond percolation in the WPSL and in the regular planar lattices.

Exponents	Regular 2D lattice	WPSL bond/site
ν	4/3	1.635
β	5/36	0.222
γ	43/18	2.825
τ	187/91	2.0728
d_f	91/48	1.864

critical exponents. All these provide a clear testament that the site and bond percolations on WPSL belong to the same universality class, which differs from the universality class where all known planar lattices belong.

It is worth noting that Corso *et al.* have also studied percolation on a multifractal planar lattice and found that it belongs to the universality class of the regular planar lattices and not of the WPSL [14]. Thus it is not the multifractal nature of the lattice which could be held responsible for the separate universality class of the WPSL. On the other hand, Hsu and Huang studied percolation on a class of random planar lattices where $P(k)$ do not follow a power law and, instead, is peaked at about $k = 6$ [13,25]. Despite all the differences from the regular planar lattices, they still found it belongs to the universality class of the regular planar lattices. In both cases, the dimension of the objects coincide with that of the space where they are embedded. Now what happens when the dimension of the object does not coincide with that of the space? The answer to this question can be found from the work of Lin *et al.,* who studied percolation on a class of Sierpinski carpet [30]. Note that the dimension of the Sierpinski carpet is always less than 2 of the plane where it is embedded. They found that the universality class differs for each different value of the fractal dimension. However, WPSL belongs to a different universality class despite that its dimension coincides with the dimension of the space where it is embedded. We hope that our findings will have a significant impact on the future study of the percolation theory.

[1] D. Stauffer and A. Aharony, *Introduction to Percolation Theory* (Taylor & Francis, London, 1994).

[2] S. R. Broadbent and J. M. Hammersley, Math. Proc. Cambr. Philos. Soc. **53**, 629 (1957).

[3] H. Dashtian, G. R. Jafari, M. Sahimi, and M. Masihi, Physica A **390**, 2096 (2011).

[4] P. G. de Gennes and E. Guyon, J. Mec. **17**, 403 (1978).

[5] S. Boccaletti, V. Latora, Y. Moreno, M. Chavez, and D. Hwang, Phys. Rep. **424**, 175 (2006).

[6] S. N. Dorogovtsev and J. F. F. Mendes, *Evolution of Networks* (Oxford University Press, Oxford, 2003).

[7] M. E. J. Newman and D. J. Watts, Phys. Rev. E **60**, 7332 (1999).

[8] R. Cohen, K. Erez, D. ben-Avraham, and S. Havlin, Phys. Rev. Lett. **85**, 4626 (2000).

[9] H. E. Stanley, *Introduction to Phase Transitions and Critical Phenomena* (Oxford University Press, Oxford, 1971).

[10] J. J. Binney, N. J. Dowrick, A. J. Fisher, and M. E. J. Newman, *The Theory of Critical Phenomena* (Oxford University Press, New York, 1992).

[11] F. Yonezawa, S. Sakamoto, and M. Hori, Phys. Rev. B **40**, 636 (1989); **40**, 650 (1989).

[12] A. M. Becker and R. M. Ziff, Phys. Rev. E **80**, 041101 (2009).

[13] H.-P. Hsu and M.-C. Huang, Phys. Rev. E **60**, 6361 (1999).

[14] G. Corso, J. E. Freitas, L. S. Lucena, and R. F. Soares, Phys. Rev. E **69**, 066135 (2004).

[15] A. A. Saberi, Phys. Rep. **578**, 1 (2015).

[16] M. K. Hassan and M. M. Rahman, Phys. Rev. E **92**, 040101(R) (2015).

[17] M. K. Hassan, M. Z. Hassan, and N. I. Pavel, New J. Phys. **12**, 093045 (2010); J. Phys.: Conf. Ser., **297**, 012010 (2011).

[18] F. R. Dayeen and M. K. Hassan, Chaos Solitons Frac. **91**, 228 (2016).

[19] G. I. Barenblatt, *Scaling, Self-similarity, and Intermediate Asymptotics* (Cambridge University Press, Cambridge, 1996).

[20] G. J. Rodgers and M. K. Hassan, Phys. Rev. E **50**, 3458 (1994).

[21] M. K. Hassan and G. J. Rodgers, Phys. Lett. A **218**, 207 (1996).

[22] P. L. Krapivsky and E. Ben-Naim, Phys. Rev. E **50**, 3502 (1994).

[23] Y. L. Luke, *The Special Functions and Their Approximations I* (Academic Press, New York, 1969).

[24] J. Feder, *Fractals* (Plenum, New York, 1988).

[25] M. M. de Oliveira, S. G. Alves, S. C. Ferreira, and R. Dickman, Phys. Rev. E **78**, 031133 (2008).

[26] M. E. J. Newman and R. M. Ziff, Phys. Rev. Lett. **85**, 4104 (2000); Phys. Rev. E **64**, 016706 (2001).

[27] R. M. Ziff, Phys. Rev. Lett. **69**, 2670 (1992).

[28] R. M. Ziff and M. E. J. Newman, Phys. Rev. E **66**, 016129 (2002).

[29] C.-K. Hu, C.-Y. Lin, and J.-A. Chen, Phys. Rev. Lett. **75**, 193 (1995).

[30] Z-Q Lin and Z. R. Yang, Commun. Theor. Phys. **27**, 145 (1997).